Title : An Instrumented Large Soil Column to Investigate Climatic Ground Interaction

Date- Revised: 01/03/2020

Author 1 :

- **Udukumburage R. S.,** (B.Sc.), PhD student in Geotechnical Engineering
- School of Civil and Environmental Engineering, Science and Engineering Faculty, Queensland University of Technology, Brisbane 4000, Queensland, Australia.
- ORCID number: 0000-0002-1762-1124

Author 2 :

- **Gallage, C.,** (PhD.), Senior Lecturer
- School of Civil and Environmental Engineering, Science and Engineering Faculty, Queensland University of Technology, Brisbane 4000, Queensland, Australia.
- ORCID number: 0000-0002-0978-9066

Author 3 :

- **Dawes, L.,** (PhD.), Professor
- School of Civil and Environmental Engineering, Science and Engineering Faculty, Queensland University of Technology, Brisbane 4000, Queensland, Australia.
- ORCID number: 0000-0003-2329-5940

Corresponding Author :

- Name : Udukumburage, R. S.,

- Contact Address : S920-7, School of Civil and Environmental Engineering, Science and Engineering Faculty, Queensland University of Technology, Brisbane 4000, Queensland, Australia.
- Contact Number : +6146479244
- Email : rajithashehan.udukumburage@hdr.qut.edu.au

Number of words in the main test excluding abstract and references: 5000 words

Number of Figures: 15

Number of Tables: 02

List of notations:

CH	-	Silty clay
USCS	-	Unified Soil Classification System
A_c	-	Activity value
SWCC	-	Soil Water Characteristic Curve
PE	-	Potential Evaporation
LVDT	-	Linear Variable Differential Transducer
RH	-	Relative Humidity
vwc	-	Volumetric water content
T	-	Temperature
θ_T	-	Volumetric water content at T °C
θ_{20}	-	Volumetric water content at 20 °C
A_{EC-5}	-	Voltage response of EC-5 sensor (V)
ε_T	-	Temperature error factor
m	-	Change in vwc for unit change in temperature corresponds to vwc of sample at 20°C

Abstract

The field monitoring of the climatic-induced behaviour of the expansive soil has always been difficult, expensive and time-consuming. The uncontrollability of the field boundary conditions and difficulty in accurately measuring them have worsened the problem. As an alternative, the instrumented model setups are ideal for long-term monitoring of expansive soils since the laboratory compacted expansive soils become environmentally stabilized after few wet-dry cycles. There had been a very limited laboratory-based column setups for the observation of expansive soils under unsaturated conditions with an appropriate set of sensors embedded at known depths. The major difficulties associated with model tests are considerable boundary effect and sensor to soil area ratio due to the insufficient physical model dimensions. In this study, the research need for a laboratory model setup with minimized boundary effects has been addressed by a large instrumented soil column which could more closely represent environmentally stabilized soil. The current results depict the expected pattern for the variations of soil suction, volumetric water content and soil displacement under wetting and drying phenomenon which accentuates the applicability of instrumented soil column for the investigation of climatic-induced expansive soil behaviour.

Keywords

Expansive soils; Model test; Monitoring; Suction; Ground movement; Wet-dry cycle; Geotechnical engineering; Partial saturation

1. Introduction

Natural expansive soils undergo cyclic drying-wetting phenomenon resulting in significant volume changes in the soil which leads to unfavourable conditions for light-weight structures founded on and in these soils. Therefore, investigation of the climatic-induced ground response has been an important geotechnical aspect to evade unfavourable results on light-weight structures (Adem & Vanapalli, 2013; Chan et al., 2009; Chan et al., 2015; Chan et al., 2016; Fityus & Smith, 1998; Fityus et al., 2004; McKeen, 1992; Overton et al., 2006; Rajeev et al., 2012; Vu & Fredlund, 2006). Designing of the foundations on expansive soils need special consideration on the swell-shrink effect due to climate changes. Generally, these foundations are designed to withstand the maximum deflection exert on the foundation due to the climatic-induced soil responses.

Even though most of these foundation issues associated with expansive soils can be overcome by over-designing the structures according to the saturated soil mechanics, which causes overestimation of design costs. Therefore, the need for a better solution has been investigated during the past few decades using the geotechnical improvements in unsaturated soil mechanics (Kuriqi et al., 2016; Muceku et al., 2016). In this regard, numerous field and laboratory-based research are presented in the literature (Chan et al., 2010; Fityus et al., 2004; Gallage et al., 2009; Gallage et al., 2012; Hu et al., 2008; Karunarathne et al., 2014; Kodikara et al., 2014; Miller & Stoker, 2008; Ng et al., 2003; Ng et al., 2008; Ng & Zhan, 2007). The major problem encountered in the field monitoring is uncontrollability of the boundary conditions and difficulty in accurately measuring them (Tang et al., 2009; Udukumburage et al., 2019). To alleviate the complexities in field studies, the laboratory-based model setups have been used by many researches due to the controlled conditions which conducive to parametric studies (Cui et al., 2008; Cui et al., 2013; Gallage et al., 2017; Schanz et al., 2013; Tang et al., 2009).

The hydro-mechanical behaviour of compacted expansive clays can be investigated through a properly designed instrumented model tests. Soil model tests on sand material are less complicated compared to expansive clay soils (Cui et al., 2013; Dadgar et al., 2018; Gallage et al., 2017; Gallage et al., 2008; Gallage & Uchimura, 2010; Pan et al., 2010; Puppala et al., 2011a; Udukumburage, 2019). When performing soil column model test on expansive soils, it is important to consider a larger diameter to minimise boundary effects and to monitor sub-soil deformation, suction, moisture content, and temperature along with the depth of the column accurately to understand its response to cyclic drying and wetting conditions. Displacement mechanism should be implemented such that sensor to soil area ratio is minimal and the settlement plate contact area is sufficient to capture the vertical soil displacement.

The available research utilized physical model sizes that may not accurately represent the field soil strata (Lewis & Sjöstrom, 2010; Liu et al., 2002; Prueger et al., 1997; Sahoo et al., 2009). Essentially, the boundary effect of the soil models has always been the major concern for the small-scaled soil columns, hence the measured soil heave is an underestimation of the actual vertical expansion. Laboratory based apparatus cannot avoid friction at the soil-wall interface; however, this friction has a minimal effect on the central part of the soil, provided the sample size (cross-section) is large. According to Sentenac et al., (2001) flow velocity around the wall can be 11% - 45% greater than that of the column centre due to increased permeability. Nevertheless, sidewall roughening or glueing sand on the internal column surface has been proven to minimize this effect (Smajstrla, 1985). According to Bergström (2000), the diameter to length ratio should be 1:4 in order to minimize the sidewall flow of a laboratory soil column. Therefore, large soil columns could represent the actual ground as proper soil compaction within the packed columns avoiding erratic soil behaviour (Tang et al., 2009). Past studies state that remoulded expansive clays tend to environmentally stabilized after several wet-dry cycles;

hence, could be used to simulate an actual ground (Chikhaoui et al., 2017; Gould et al., 2011; Kodikara et al., 2018; Wang & Wei, 2014; Zhao et al., 2017).

However, due to the issues mentioned, limited research has been carried out for long term monitoring of expansive clays using methodically calibrated set of sensors (Feng, et al., 2002; Manju et al., 2008; Puppala et al., 2011b; Tarantino et al., 2008; Wu et al., 2018). The knowledge gathered from the field investigations of climate-ground interaction in expansive soils suggest that the long-term monitoring of the top 1 m would provide a clear understanding about the hydro-mechanical responses of expansive soils (Fityus et al., 2004; Karunarathne et al., 2014; Miller & Stoker, 2008). Therefore, an instrumented expansive soil model which is at least 1 m high can be considered as a large physical model that may represent an actual ground. However, a limited number of large expansive soil monitoring setups can be found in the literature. Apart from that, current studies focus on either wetting or drying phenomenon of expansive soils (Cui et al., 2013; Tang et al., 2009); however, limited studies emphasized the effect of a single wet-dry cycle (Gallage et al., 2017). More importantly, extremely limited model studies have investigated the effect of climatic-induced ground response in expansive soils for multiple wet-dry cycles (Amenuvor et al., 2018).

It is important to understand that the compacted expansive soils may represent actual ground (in-situ) conditions after they have environmentally stabilized (Zhao et al., 2017). To achieve this, expansive soil specimen is required to subject into several wet-dry cycles according to Kodikara et al. (2018). Therefore, it is important to develop such geotechnical instruments which can be used to monitor climatic-induced ground movement under controlled conditions. The main features of long-term operability, a representative size of the actual ground and, the capability to determine the active zone depth and resultant surface movements, differentiate these geotechnical instruments from the simple element scale tests. Hence, the main objective of this study is to develop a long-term operable instrumented soil column which has the dimensions of 1 m in height and 0.4 m in diameter to investigate climatic induced ground response. The imperative soil parameters for the investigation are sub-soil displacement, soil moisture content and soil suction. This study will highlight the laboratory monitoring of moisture, suction and displacement profiles of expansive soil and evaluate the pertinence of a large instrumented soil column to investigate climatic induced ground responses. The responses are measured at different soil depths to understand the effect of wetting and drying on hydro-mechanical responses of the system. This overall system (i.e. geotechnical instrument) is capable of determining the active zone depth and resultant surface movement of expansive clay for given climatic conditions, unlike element scale tests (i.e. Oedometer based swell-shrink tests).

2. Materials and method

2.1 Testing Material

Natural expansive grey clay collected from Sherwood, Queensland in Australia was used in this study. These grey Vertosol soils are widespread in southeast Queensland region and representative of subsoil conditions in Brisbane. Table 1 shows the basic properties of the soil and it is classified as CH (Clay of High Plasticity) according to the Unified Soil Classification System (USCS). Figure 1 depicts the Soil-Water characteristic curve (SWCC) of the soil obtained for the wetting path from different suction measuring methods: tensiometer (0 – 90 kPa), water potential sensors – MPS6 (100 kPa – 4000 kPa) and WP4C Dewpoint Potentiometer – Psychrometer (4 MPa – 30 MPa).

[Table 1]

[Figure 1]

2.2 Soil column and measuring devices

The soil column apparatus shown in figure 2 consists of an acrylic tube, a PVC base plate, and an LVDT mounting plate. The internal diameter of the 1.2 m long acrylic tube is 390 mm and its wall thickness is 5 mm. Both ends of the tube were attached to annular rings with an outer diameter of 480 mm. Holes 5 to 10 mm in diameter were drilled along the length of the tube to take the sensor cables out of the soil column. The 480 mm diameter PVC base plate was machined to have two drainage ports and a 150 mm diameter recess at the centre to place a bronze porous disc. An LVDT mounting plate is attached to the top annular ring of the soil column.

[Figure 2]

In this study, the deformation of the sub-soil was captured at five specified levels. The soil moisture variations were captured using two types of moisture sensors (i.e. MP406 and EC5) at five different soil levels. High and low suction changes were carefully measured by methodically embedded water potential sensors and tensiometers, respectively. Calibrated thermistors were placed at six different locations to obtain the subsoil temperature profile. The environmental parameters such as relative humidity (RH) and ambient temperature (T) were monitored throughout using a weather station setup. An evaporation pan (diameter = 390 mm) of having the same diameter as the column setup was used to monitor the potential evaporation (PE) of water. The sensor calibration process and column setup are comprehensively discussed below.

2.2.1 Soil moisture sensors

To measure volumetric water content (vwc) of the soil, five dielectric moisture sensors (EC-5) and four 'Time Domain Reflectometers' (TDR – MP406) were used. Two types of sensors for moisture measurements were used to investigate the consistency of the sensors in long-term monitoring of expansive Vertosol soils. MP406 sensors were used as the primary source of volumetric water content due to the stability and reliability of sensor responses (not affected by temperature or soil salinity). EC5 sensors were embedded as backup monitoring source for long-term operation of the soil column. Each sensor was calibrated in the test material.

Since EC-5 moisture measurements are very sensitive to temperature, temperature correction factors were developed by measuring soil moisture at different temperatures. The soil samples with five different known gravimetric moisture contents (i.e. 15%, 20%, 25%, 30% & 35%) were static compacted to achieve dry density of 1.2 g/cm^3 (field density). A calibrated temperature sensor (Therm-EP) was embedded to acquire the temperature variation throughout the measuring duration. Soil moisture was maintained constant during the experimentation by applying a thick grease layer on the topsoil surface. The final gravimetric moisture content of the soil was measured by oven drying the test sample to make sure the moisture is successfully maintained.

[Figure 3]

The results indicated a significant variation of dielectric responses of EC-5 moisture sensors when the temperature varies from 15 °C to 33 °C during heating and cooling cycles (Figure 3a).

$$\theta_T = \theta_{20} - \varepsilon_T\ (m, \Delta T)$$

$$\theta_T = (1.383 \times A_{EC\text{-}5} - 1.0868) - \varepsilon_T (m, \Delta T)$$

$$\theta_T = (1.383 \times A_{EC\text{-}5} - 1.0868) - [m \times (T-20)] \quad (1)$$

Where;

θ_T = Volumetric water content at T °C

θ_{20} = Volumetric water content at 20 °C

$A_{EC\text{-}5}$ = Voltage response of EC-5 sensor (V)

ε_T = Temperature error factor

m = Change in vwc for unit change in temperature corresponds to vwc of sample at 20 °C

The temperature calibration was conducted with respect to T = 20 °C and 'm' value for equation (1) can be determined from figure 3b provided that volumetric water content of the soil at 20 °C is known. Equation (2) shows the statistical relationship obtained between the 'volumetric water content of the soil at 20 °C' and 'change in vwc for a unit change in temperature' that can be used to derive equation (3); temperature calibrated volumetric water content of EC5.

$$m = 0.0074 \times \theta_T + 0.0002 \quad (2)$$

$$\theta_T = (1.383 \times A_{EC\text{-}5} - 1.0868) - [\{0.0074 \times \theta_T + 0.0002\} \times (T-20)]$$

$$\theta_T = (1.383 \times A_{EC\text{-}5} - 1.0868) - [\{0.0074 \times (1.383 \times A_{EC\text{-}5} - 1.0868) + 0.0002\} \times (T-20)] \quad (3)$$

The same methodology was used to calibrate MP406 sensors for the range of gravimetric water contents (15% - 35%) and field density (dry density = 1.2 g/cm^3); however, no temperature calibration was performed due to the temperature independency of the MP406 sensor responses.

2.2.2 Soil suction sensors

Two types of sensors (a laboratory-designed tensiometer and a water potential sensor) were employed to measure matric suction in the soil column test (figure 4). The laboratory-designed tensiometers were used to measure matric suctions of up to 90 kPa. As shown in figure 5a, this tensiometer was designed to flush out air bubbles formed in the ceramic cup to enable the long-term use of the sensor. The Aluminium block to which the pressure transducer was connected, was mounted on the outer wall of the soil column. The ceramic cup, with an air-entry value of 1 bar (100 kPa) was placed in soil.

[Figure 4]

The MPS6 sensor consists of water content sensors surrounded by two porous ceramic discs. When the sensor with saturated porous discs is installed in the soil, the water in the porous disc equilibrates with the soil moisture, achieving the matric suction in the porous disc, which is the same as the soil's matric suction. At this stage, the water content in the ceramic disc is measured by the water content sensors and it is converted to matric suction by using the water retention curve of the porous disc (figure 4b). This water retention curve of the sensor was provided by the manufacturer based on mercury intrusion porosimetry data; hence, MPS6 sensors were factory calibrated for EM50 dedicated data logging system (Tripathy et al., 2016). Irrespective of hysteresis in drying and wetting paths present, the manufacturer has experimentally found that the magnitude of hysteresis error is less than 10% when measured suction is less than 100 kPa. Therefore, hysteresis was not taken into account in the specified SWCC for MPS6 sensor. Thermistor embedded on MPS6 sensor provides the corresponding temperature for each suction measurement. EM50 responses for MPS6 sensors are factory calibrated for temperature (Tripathy et al., 2016). Four MPS6 sensors used in this study were factory-calibrated with six-point calibration using the dedicated logging system to give the soil matric suction in kPa. According to the manufacturer specification, the measurable range of the sensor is from 9 to 100,000 kPa. However, Tripathy et al. (2016) experimentally showed MPS6 sensors can measure very high suctions up to 10,000 kPa and very low suctions down to 9 kPa in expansive clays. The response time mentioned in manufacturer specification is 150 milliseconds.

2.2.3 Sub-Soil Displacement

Five settlement plates embedded at selected depths were used to measure the sub-soil deformation. As shown in figure 5a, each settlement plate (100 mm diameter, 10 mm thick Aluminium plate) was attached with a shaft that runs through a PVC sleeve to above the soil surface (settlement plate area to soil area ratio = 6.5%). PVC guiding sleeve is not rigidly connected to the settlement plate and rod attachment to minimize the interference to vertical soil displacement. The smooth outer surface of PVC sleeve which in contact with the soil provides minimal resistance to vertical soil displacement. At the top, the shaft movement is guided by a guiding block and an LVDT sitting on the top of the shaft measure the vertical movement of the shaft. The vertical movement of the shaft directly represents the soil movement at the depth where the plate is embedded. All five LVDTs (measuring range of 0 - 100 mm) were pre-calibrated attached to the data logging system.

[Figure 5]

As a secondary method of tracking the sub soil displacement, the level indicators (figure 5b) were embedded at known locations (50 mm soil lifts) at an angle of 90° apart, which enables further investigation of the peripheral soil movement as well. The markers were coated with oil-based white paint in order to increase the durability and visibility for long term monitoring purpose. Vertical soil displacements at the soil-acrylic boundary (peripheral) and the mid part of the soil were monitored at different depths using level indicators and LVDT-settlement plate attachments respectively. Effect of friction between the chamber wall and soil can be determined by comparing the displacement values at the chamber boundary and mid soil. Heat exchange between the ambient air and the soil strata was assumed negligible in this study (Tang et al., 2009; Cui et al., 2013).

2.2.4 Sub-soil and Atmospheric Temperature

In this study, five temperature sensors (Therm-EP) were embedded at different sub-soil levels in order to monitor the soil temperature profile. The temperature sensors were calibrated within the experimental room temperature range (20 °C to 40 °C) and extrapolated to obtain any other temperature using a highly correlated (R^2 = 0.99) regression equation. In this study, temperature measurements were only used to get the calibrated EC-5 moisture values.

2.2.5 Climate Conditions

The climate conditions around the soil column were monitored by evaporation pan (Potential Evaporation), VP4 (Relative Humidity) and Therm-EP (Air Temperature) sensors. Evaporation pan (figure 6a) has the same diameter (Inner diameter = 390 mm) as the soil column and calibrated level sensor is installed to monitor the change in water height of the pan. Potential evaporation (mm/day) of the water from the soil column is equivalent to the evaporated water height that can be determined from the evaporation pan unit. The calibration chart for the level sensor is shown in figure 6b. Environmental monitoring unit placed closer to the soil column provides the relative humidity (RH) and air temperature of the surrounding area as shown in figure 8.

[Figure 6]

3. Setting up of the soil column & wet-dry simulation

Initially, a fine sand layer was compacted at the base of the soil column up to 30 mm layer thickness (figure 7a) to provide sufficient bottom drainage. A geo-fabric layer (figure 7b) was placed on top of it, in order to separate the sand and clay layers. Subsequently, 8.242 kg of wet soil (G.W.C = 15%) was poured into the acrylic column and compacted to a 50 mm of layer thickness to achieve the target dry density of 1.2 g/cm^3 (figure 7c). The dry density of 1.2 g/cm^3 has used this investigation as it was the average in-situ density value measured in the area where the test material was procured. This density controlled wet-compaction was repeated to achieve 1000 mm soil height in the column. Table 2 shows the type of sensors and the depths at which they were installed during the preparation of the soil column.

[Figure 7]

[Table 2]

The inner side of the acrylic column was kept slightly rough to avoid preferential water flow at soil-acrylic contact boundary once the water is supplied (Smajstrla, 1985). This process will induce some amount of interface friction at the boundary. However, authors used two different mechanisms to monitor the soil displacement at the boundary and at the mid part of the soil layer to investigate the friction effect at the boundary. Tang et al. (2009) used the same approach to investigate edge friction at the surface. LVDT-settlement plate attachments were placed at different depths (table 2); however, closer to the centre of the soil column to capture the soil displacement around the centre. Level indicators were placed at every 50 mm soil lift (figure 5b) to observe peripheral soil displacements and thereby investigate the correlation between the mid and boundary soil movements.

The instrumented soil column (figure 8b) was subjected to a complete wetting cycle (until no further significant heave; heave < 0.5 mm per month) by maintaining a constant ponding water level of 50 mm at the top of the soil column using a Mariotte's bottle. This induced slow wetting process is helpful to monitor the hydro-mechanical responses in soil. The Mariotte's bottle can maintain the water level in the column at the same level where the tip of the inner tube is located. The water in the Mariotte's bottle above the tip of the inner tube is the storage to provide water to the column to compensate for infiltrating water along the soil column.

The moisture, suction and temperature profiles of the soil accompanied with the subsoil movement were monitored through the sensor responses from each predefined sensor embedded levels (figure 8a). All the sensor responses were recorded via a dedicated data logger and the real-time sensor responses were observed. The data acquisition interval (data resolution) was set to 1 minute to observe the slightest variation in sensor responses. Vertical movements of the level indicators were constantly monitored and compared with the LVDT sensor responses.

[Figure 8]

Subsequent to 160 days of the constant head wetting period, two 100 kW heat lamps were attached at a location which is equidistant to both soil column and evaporation pan. The main reason to use the heat lamp setup is to accelerate the drying process under controlled conditions. The distance between the centre of the topsoil surface and the heat lamps was 0.5 m; therefore, induced heat increased the air/soil temperature to a realistic value in Brisbane (without exceeding 36 °C in summer). Potential evaporation (PE) of expansive soil was captured using the evaporation pan (figure 9). The drying cycle was imposed on the soil column for 165 days until the soil reaches steady-state condition. The constant head water table was maintained at the bottom of the soil column using a water container attached to a Mariotte's bottle as shown in figure 9. Moisture, suction, temperature and subsoil movements were captured using the embedded set of sensors during the imposed drying period.

[Figure 9]

4. Results and discussion

4.1 Volumetric moisture profile during wet-dry cycle

The moisture sensor responses of the instrumented soil column depicted predictable results during the first wet cycle as shown in figure 10. Temporal variations of moisture sensor responses reached a plateau and positive pore water pressure indicated by the tensiometer at 800 mm depth implied hydraulic steady-state condition of the soil. Temporal variation of EC5 vwc responses is shown in figure 10b to display the instability of these sensors. The mechanical behaviour of expansive soil was also a critical factor to select the wetting period as soil expansion is a time-dependent phenomenon (Nelson, 2015).

[Figure 10]

The initial MP406 responses at the depths of 50 mm, 150 mm, 300 mm and 800 mm (from the surface) were 17.1%, 19.6%, 18.6% and 17.1%, respectively. The vwc of the top 300 mm reached to an equilibrium in t=4 days, whereas the moisture sensor at 800 mm (from the surface) equilibrated after t=160 days. Saturated vwc of the soil profile, ranged from 46% - 50% due to the entrapped air during the wetting process (Siemens et al., 2014). Volumetric water content profiles from EC5 and MP406 represented a close match up to 25 days at 30 mm, 50 mm and 800 mm depths. After the EC5 sensor failures at 150 mm and 500 mm levels, EC5 responses were not consistent with MP406 responses.

After wetting, the soil column was subjected to a drying period of 165 days and initial vwc profile of the soil column was shifted towards the left side as shown in figure 11a. The decrease in vwc was prominent from the topsoil surface and up to 300 mm depth of the column. VWC of the soil at 50 mm depth from the surface depicted a drastic decrease from 49.2% to 17.4% where it reached the steady-state condition. Variation in vwc at 150 mm level was observed from 48.8% to 43.6% until the steady-state condition was reached and insignificant change in vwc (< 0.5%) at 800 mm level depicts the effect of the drying front diminishing with soil depth. Figure 11b shows the temporal distribution of EC5 vwc at embedded depths in drying process which demonstrated good consistency with MP406 responses compared to the wetting process.

[Figure 11]

4.2 Soil suction profile during wet-dry cycle

Variation in MPS6 soil suction profile during the wetting process is shown in figure 12a. Initial suction profile demonstrated a slight variation with soil depth and suction at top 300 mm decreased to 11 kPa when the wetting fronts reached down to 300 mm from the surface after 3 hours. Subsequently, all the suction sensors displayed value of 9 kPa to 10 kPa at t = 4 days, which eventually equilibrated at 7 kPa after t = 160 days. Figure 12b shows the temporal variation of the tensiometer responses during the wetting process. Responses at 300 mm and 800 mm levels are displayed as other two tensiometers encountered technical failure at the beginning. However, soil suction of 7 kPa after t = 160 days seems to be an overestimation of 7 kPa when compared to low suction tensiometer unit responses. Tripathy et al. (2016) experimentally showed minimum suction in clay that can be measured using MPS6 sensor is 9 kPa and reflects the saturated condition. Full saturation of soil was verified by the positive tensiometer response monitored at 800 mm soil depth.

[Figure 12]

Variations in MPS6 suction profile during the drying process is shown in figure 13a. Most critical variation in suction (7 kPa to 1800 kPa) was observed at 50 mm level during the drying period. Desiccation at 150 mm level resulted in a considerable increase of suction 8 kPa to 43 kPa. At the soil depth of 300 mm, the observed suction variation was increased from 9 kPa to 18 kPa during the drying period. According to tensiometer responses in Fig 13b, it can be deduced that tensiometer at 300 mm depth verifies MPS6 response after 165 days of the operational period. Significant inconsistency was observed in tensiometer responses at 300 mm depth until flushing out air at t = 130 days. Overall, the active zone depth of the soil (AS2870, 2011) can be deemed as 500 mm from the topsoil surface as illustrated in figure 13a.

[Figure 13]

Figure 14 compares the laboratory determined SWCC with the matric suction and corresponding volumetric water content values directly obtained from the MPS6 and MP406 sensors in the soil column during wetting and drying processes. The laboratory determined SWCC depicts a reasonably good agreement with direct measured soil suction-vwc data during wet-dry processes of the column and similar observation was made by Gallage et al. (2017). This verifies that the proposed soil column setup can be used to simulate soil-climatic interactions following the laboratory determined properties (e.g. SWCC). Water content sensors have less response time compared to suction sensors. Therefore, an error can be included when considering a suction value corresponding to a particular water content in a rapidly changing environment (e.g. at the approach of the wetting front).

[Figure 14]

4.3 Sub-soil displacement during wet-dry cycle

Subsoil movements monitored during the wetting process is shown in figure 15a. At the outset of the wetting cycle, the LVDT responses depicted a heaving (positive deformation) from the surface up to 300 mm column depth and a slight settlement at 500 mm (negative deformation) level. This negative deformation at 500 mm level is only present in LVDT readings; however, cannot be identified from the peripheral movements captured by level indicators. The main reason for such behaviour could be the increased overburden due to wetting, but this is not reflected at 800 mm depth. Further, wetting of the shallow soil layer induces swelling pressure to deeper layers due to the friction between the shallow layer and the column wall. This phenomenon was not reflected in the displacement responses at 800 mm soil depth as it is too far from the top.

[Figure 15]

The peripheral soil movements captured by the embedded level indicators inferred a reasonable agreement with the LVDT measured inner subsoil movements (as depicted in figure 15). The surface movements captured by the markers provided a greater value compared to the LVDT based measurements since self-weight of the aluminium settlement plates hinders the free swell at the soil surface. However, the subsoil displacements observed by the markers (peripheral) provided a slightly lower displacement in comparison with the LVDT readings due to friction between the soil and column at the boundary. The effect of the soil-wall friction on the displacement measurements is minimised in this study by considering a large cross-sectional area and placement of the primary displacement monitoring units at the centre. Overall, the observed heaving at the centre provided a greater displacement compared to the peripheral soil movements. Vertical soil displacement at the boundary is almost half as the central displacements below surface levels; implying the diminishing effect of soil-wall friction on the vertical displacement in a large soil column. Therefore, the centrally located primary displacement monitoring units have served their purpose by minimising the friction effect. Findings of the current study align with the boundary and central displacement findings of Tang et al (2009).

During the drying process, evaporation of water associated with expansive soil resulted in significant vertical shrinkage at the topsoil surface (11.8 mm after 165 days) as shown in figure 15b. More than two-thirds of the vertical shrinkage occurred during the initial 25 days of the drying period. At 150 mm depth, the observed vertical shrinkage amounts to 2.5 mm after soil reached the steady-state condition. From 300 mm level and below, positive, but minimal soil displacements (< 1 mm) were observed due to the release of surcharge from the soil above during the desaturation process. The level indicator movements for the analysis of peripheral displacements for the top 150 mm due to the disturbance caused by lateral shrinkage of soil. Therefore, the results presented here are purely based on the LVDT responses. However, the level indicators reflected 0 mm movement from 300 mm level onwards. Therefore, collective observations of level indicators and LVDT responses deduce that release of surcharge during the drying process mainly affects the inner soil compared to the soil at the boundary.

4.4 Applicability of the setup

The long-term operable soil column presented in this study has many advantages over other apparatus. Most soil model test apparatus presented in literature tested for sand; however, limited studies can be found for expansive soils (Cui et al., 2013; Cui et al., 2016; Gallage et al., 2017; Tang et al., 2009). From field and laboratory studies, 1m high soil specimen have been found to be sufficient to investigate the climatic-induced ground response of expansive soils (Amenuvor et al., 2018; Cui et al., 2013; Laporte et al., 2018; Ng et al., 2016; Tang et al., 2009) and more accurately replicates the field conditions. Subsoil displacement is an important parameter to investigate the behaviour of expansive soils; however, is not considered in the previous studies. The proposed setup is novel in long-term operability, optimised dimensions and monitoring techniques of subsoil responses. This setup has the capability of monitoring the long-term variations in subsoil displacements at the boundary and the central part of the expansive soil. This is useful to investigate the effect of soil-wall friction on subsoil displacement. Further, monitoring of subsoil allows identifying the active zone depth of the soil profile that contributes to the surface displacement. The long-term operability of the soil column is ensured by the availability of backup displacement and moisture monitoring mechanisms.

The main drawback of this apparatus is the lateral shrinkage monitoring mechanism. From the subsoil displacement responses at the boundary and the centre, it was deduced that soil-wall friction at 150 mm depth was considerable. The same behaviour was observed (at the surface) by Tang et al. (2009); where the central heave was determined as double the displacement observed at the boundary. Less reliable and inconsistent performance of secondary moisture monitoring mechanism (EC5) was observed. Low capacity and inconsistencies were observed in the low suction tensiometer units due to the long water reservoir in tensiometer tubes which underestimated the water tension due to soil suction. Further, long equilibrium time of the tensiometers may produce inconsistencies under infiltration conditions as mentioned by Tang et al. (2009).

The instrumented soil column is not insulated and hence, the temperature fluctuations at the surrounding affect the soil profile. The temperature gradient between the surrounding and the soil is negligible when compared to the effect of the heat-lamp induced heat on the topsoil (as expected). This temperature difference between the inner and outer sides of the acrylic (10 mm thick) has negligible heat transfer characteristics due to the very low thermal conductivity of acrylic (0.2 W/m.K). Therefore, heat exchange between the soil and the atmosphere from the sides of the soil column is not considered.

5. Conclusion

The instrumented soil column was successfully operated for a total period of 325 days which consist of 160 days of wetting and 165 days of drying. Soil suction variations were successfully captured by MPS6 sensors and tensiometer units were utilized to verify the hydraulic steady-state condition. Subsoil displacements of the expansive soil during wetting depicted greater peripheral movement when compared to the inner soil at the topsoil surface due to free swelling and inner soil movement is slightly hindered by the self-weight of settlement plate connected to LVDT attachment. At all the other depths, boundary displacement is slightly lower than that of inner soil due to the soil-acrylic interface friction. Further investigation on the soil-acrylic interface friction requires a series of direct shear tests for selected water content and surcharge conditions.

Surface movements were the prominent variation during both wetting (inner displacement = 38.1 mm, peripheral movement = 45 mm) and drying periods (inner displacement =11.8 mm). Level indicators were successful in measuring the peripheral soil movement during the wetting period; however, were not helpful to measure boundary movements during drying cycle due to disturbance caused by lateral shrinkage. The active zone depth of the soil column can be considered as 300 mm from the topsoil surface after the wet-dry period of 325 days. The 'top 50% of the active zone depth' (i.e. 150 mm) has contributed to 60% and 80% of the total vertical displacement in wetting and drying processes respectively. This study accentuates the applicability of the large instrumented soil column to investigate the reactive zone depth and climatic-induced ground movement of grey Vertosol soil. The methodology can be modified to investigate the climate-ground interaction of other expansive soils under controlled laboratory conditions.

Acknowledgements

Authors gratefully acknowledge the technical staff at Queensland University of Technology (QUT) for providing the on-campus & off-campus (Banyo Pilot Plant) support to conduct this soil column test. Further, the gratitude should be extended to Steven Hackworth from 'The SoilTesters' for providing soil for this project. The first author acknowledges the scholarship for the doctoral degree received from QUT, Australia.

References

Adem, H.H. and Vanapalli, S.K., 2013. Constitutive modeling approach for estimating 1-D heave with respect to time for expansive soils. *International Journal of Geotechnical Engineering*, 7(2), pp.199-204.

Altafi-Dadgar, M., Nakhaei, M., Porhemmat, J., Biswas, A. and Rostami, M., 2018. Transient potential groundwater recharge under surface irrigation in semiarid environment: An experimental and numerical study. *Hydrological processes*, 32(25), pp.3771-3783.

Amenuvor, A.C., Li, G.W., Hou, Y.Z. and Chen, W., 2018. Shrinkage Cracking in Physical Model of Undisturbed Expansive Clay Slope subjected to Wet-Dry Cycles. In *Procedings of 7th International Conference on Unsaturated Soils*, Hong Kong.

AS 1289 – 2009 -Methods of testing soils for engineering purposes—Soil classification tests. SAI Global.

Boynton, S.S. and Daniel, D.E., 1985. Hydraulic conductivity tests on compacted clay. *Journal of Geotechnical Engineering*, 111(4), pp.465-478.

Bronswijk, J.J.B., 1988. Modeling of water balance, cracking and subsidence of clay soils. *Journal of Hydrology*, 97(3-4), pp.199-212.

Chan, D., Gallage, C., Gould, S., Kodikara, J., Bouazza, A. and Cull, J., 2009. Field instrumentation of a water reticulation pipe buried in reactive soil. *OzWater' 09 Conference Proceedings*, pp. 1-8.

Chan, D., Gallage, C.P.K., Rajeev, P. and Kodikara, J., 2015. Field performance of in-service cast iron water reticulation pipe buried in reactive clay. *Canadian Geotechnical Journal*, 52(11), pp.1861-1873.

Chan, D., Rajeev, P., Gallage, C. and Kodikara, J., 2010. Regional field measurement of soil moisture content with neutron probe. In *Proceedings of The Seventeenth Southeast Asian Geotechnical Conference*, 1, pp. 92-95.

Chan, D., Rajeev, P., Kodikara, J. and Gallage, C., 2015. Field performance of in-service cast iron gas reticulation pipe buried in reactive clay. *Journal of Pipeline Systems Engineering and Practice*, 7(2), p.04015025.

Chikhaoui, M., Belayachi, N., Nechnech, A. and Hoxha, D., 2017. Experimental Characterization of the Hydromechanical Properties of the Gypsum Soil of Sebkha of Oran. *Periodica Polytechnica Civil Engineering*, 61(4), pp.706-717.

Cui, Y.J., Ta, A.N., Hemmati, S., Tang, A.M. and Gatmiri, B., 2013. Experimental and numerical investigation of soil-atmosphere interaction. *Engineering Geology*, 165, pp.20-28.

Cui, Y.J., Tang, A.M., Mantho, A.T. and De Laure, E., 2008. Monitoring field soil suction using a miniature tensiometer. *Geotechnical Testing Journal*, 31(1), pp.95-100.

Feng, M., Fredlund, D.G. and Shuai, F., 2002. A laboratory study of the hysteresis of a thermal conductivity soil suction sensor. *Geotechnical Testing Journal*, 25(3), pp.303-314.

Fityus, S. and Smith, D.W., 1998. A simple model for the prediction of free surface movements in swelling clay profiles. In *Proceedings, 2nd International Conference on Unsaturated Soils*, Beijing, China, pp. 473-478.

Fityus, S.G., Smith, D.W. and Allman, M.A., 2004. Expansive soil test site near Newcastle. *Journal of Geotechnical and Geoenvironmental Engineering*, 130(7), pp.686-695.

Gallage, C., Chan, D., Gould, S. and Kodikara, J., 2009. Behaviour of an in-service cast iron water reticulation pipe buried in expansive soil. In *Ozwater' 09: Australia's National Water Conference and Exhibition*.

Gallage, C.P.K. and Uchimura, T., 2010. Effects of dry density and grain size distribution on soil-water characteristic curves of sandy soils. *Soils and Foundations*, 50(1), pp.161-172.

Gallage, C.P., Kodikara, J.K., Chan, D. and Davis, P., 2008, October. A comparison of the results of the numerical analysis and the physical behavior of a pipe buried in reactive clay. In *Proc., 12th Int. Conf. of Int. Association for Computer Methods and Advances in Geomechanics*.

Gallage, C.P.K., Chan, D. and Kodikara, J., 2012. Response of a plastic pipe buried in expansive clay. In *Proceedings of the Institution of Civil Engineers-Geotechnical Engineering*, 165(1), pp.45-57.

Gallage, C., Tehrani, K. and Williams, D., 2017. Instrumented large soil-column to investigate climate-induced ground deformation in expansive soil. In *Proceedings of the 19th International Conference on Soil Mechanics and Geotechnical Engineering*, Seoul, pp. 1147-1150.

Gallage, C., Udukumburage, R., Uchimura, T. and Abeykoon, T., 2017. Comparison of direct and indirect measured soil-water characteristic curves for a silty sand. *International Journal of GEOMATE*, 13(39), pp.9-16.

Gould, S.J., Kodikara, J., Rajeev, P., Zhao, X.L. and Burn, S., 2011. A void ratio–water content–net stress model for environmentally stabilized expansive soils. *Canadian Geotechnical Journal*, 48(6), pp.867-877.

Hu, Y. and Azam, S., 2008, September. Instrumentation for field monitoring in expansive soils. In *61st Canadian Geotechnical Conference*, Edmonton, Canada.

Karunarathne, A.M.A.N., Sivaner, S., Gad, E., Disfani, M., Rajeev, P., Wilson, J. and Li, J., 2014. Field and laboratory investigation of an expansive soil site in Melbourne. *Australian Geomechanics Journal*, 49(2), pp.85-93.

Kodikara, J., Rajeev, P., Chan, D. and Gallage, C., 2013. Soil moisture monitoring at the field scale using neutron probe. *Canadian Geotechnical Journal*, 51(3), pp.332-345.

Kodikara, J., Islam, T. and Sounthararajah, A., 2018. Review of soil compaction: History and recent developments. *Transportation Geotechnics*, 17, pp.24-34.

Kuriqi, A., Ardiçlioglu, M. and Muceku, Y., 2016. Investigation of seepage effect on river dike's stability under steady state and transient conditions. *Pollack Periodica*, 11(2), pp.87-104.

Laporte, S., Siemens, G.A. and Beddoe, R.A., 2018, July. Physical modelling of roads in expansive clay subjected to wetting-drying cycles. In Physical Modelling in Geotechnics, Volume 1: *Proceedings of the 9th International Conference on Physical Modelling in Geotechnics* (ICPMG 2018), July 17-20, 2018, London, United Kingdom (p. 175).

Lewis, J. and Sjöstrom, J., 2010. Optimizing the experimental design of soil columns in saturated and unsaturated transport experiments. *Journal of contaminant hydrology*, 115(1-4), pp.1-13.

Liu, C., Zhang, X. and Zhang, Y., 2002. Determination of daily evaporation and evapotranspiration of winter wheat and maize by large-scale weighing lysimeter and micro-lysimeter. *Agricultural and Forest Meteorology*, 111(2), pp.109-120.

McKeen, R.G., 1992. A model for predicting expansive soil behavior. In *International conference on expansive soils* (pp. 1-6).

Miller, S.M. and Stoker, R.C., 2008. Geotechnical and environmental indicators for characterizing expansive soils. In *GeoCongress 2008: Geosustainability and Geohazard Mitigation* (pp. 263-270).

Muceku, Y., Korini, O. and Kuriqi, A., 2016. Geotechnical analysis of hill's slopes areas in heritage town of Berati, Albania. *Periodica Polytechnica Civil Engineering*, 60(1), pp.61-73.

Ng, C.W.W. and Zhan, L.T., 2007. Comparative study of rainfall infiltration into a bare and a grassed unsaturated expansive soil slope. *Soils and foundations*, 47(2), pp.207-217.

Overton, D.D., Chao, K.C. and Nelson, J.D., 2006. Time rate of heave prediction for expansive soils. In GeoCongress 2006: *Geotechnical Engineering in the Information Technology Age* (pp. 1-6).

Pan, H., Qing, Y. and Pei-yong, L., 2010. Direct and indirect measurement of soil suction in the laboratory. *Electronic Journal of Geotechnical Engineering*, 15(3), pp.1-14.

Prueger, J.H., Hatfield, J.L., Aase, J.K. and Pikul, J.L., 1997. Bowen-ratio comparisons with lysimeter evapotranspiration. *Agronomy Journal*, 89(5), pp.730-736.

Puppala, A.J., Manosuthkij, T., Nazarian, S., Hoyos, L.R. and Chittoori, B., 2012. In situ matric suction and moisture content measurements in expansive clay during seasonal fluctuations. *Geotechnical Testing Journal*, 35(1), pp.74-82.

Rajeev, P., Chan, D. and Kodikara, J., 2012. Ground–atmosphere interaction modelling for long-term prediction of soil moisture and temperature. *Canadian Geotechnical Journal*, 49(9), pp.1059-1073.

Sahoo, D.C., Madhu, M. and Khola, O.P.S., 2009. Estimation of evapotranspiration and crop co-efficient of carrot (Daucus carota) for water management using weighing lysimeter. *Indian Journal of Agricultural Sciences*, 79(12), pp.968-971.

Schanz, T., Nguyen-Tuan, L. and Datcheva, M., 2013. A column experiment to study the thermo-hydro-mechanical behaviour of expansive soils. *Rock mechanics and rock engineering*, 46(6), pp.1287-1301.

Siemens, G.A., Take, W.A. and Peters, S.B., 2014. Physical and numerical modeling of infiltration including consideration of the pore-air phase. *Canadian Geotechnical Journal*, 51(12), pp.1475-1487.

Smajstrla, A.G., 1985. A field lysimeter system for crop water use and water stress studies in humid regions. In *Proceedings-Soil and Crop Science Society of Florida* (USA).

Tang, A.M., Ta, A.N., Cui, Y.J. and Thiriat, J., 2009. Development of a large-scale infiltration tank for determination of the hydraulic properties of expansive clays. *Geotechnical Testing Journal*, 32(5), pp.385-396.

Tarantino, A., Ridley, A.M. and Toll, D.G., 2008. Field measurement of suction, water content, and water permeability. *Geotechnical and Geological Engineering*, 26(6), pp.751-782.

Udukumburage, R.S., Gallage, C. and Dawes, L.A., 2018. Loaded swell tests to estimate the heave of the expansive soil in instrumented soil column. In *Proceedings of the 8th International Conference on Geotechnique, Construction Materials and Environment*, GEOMATE, pp.390-395.

Udukumburage, R.S., Gallage, C. and Dawes, L., 2019. Oedometer based estimation of vertical shrinkage of expansive soil in a large instrumeted soil column. *Heliyon*, 5(9), p.e02380.

Udukumburage, R.S., 2019. Laboratory based parametric study on the swell responses in expansive vertosols. *International Journal of GEOMATE*, 17(64), pp.185-191.

Vu, H.Q. and Fredlund, D.G., 2006. Challenges to modelling heave in expansive soils. *Canadian Geotechnical Journal*, 43(12), pp.1249-1272.

Wang, G. and Wei, X., 2014. Modeling swelling–shrinkage behavior of compacted expansive soils during wetting–drying cycles. *Canadian Geotechnical Journal*, 52(6), pp.783-794.

Wu, K., Wang, Y., Yu, Y., Cui, S. and Zhang, Q., 2018. Deformation Law of Surrounding Rock of Expansive Soil Tunnel Based on Dry–Wet Cycle Model Test. In *Civil Infrastructures Confronting Severe Weathers and Climate Changes Conference*, pp. 47-65.

Zhao, N.F., Ye, W.M., Chen, Y.G., Chen, B. and Cui, Y.J., 2019. Investigation on swelling-shrinkage behavior of unsaturated compacted GMZ bentonite on wetting-drying cycles. *Bulletin of Engineering Geology and the Environment*, 78(1), pp.617-627.

List of Figure Captions –

List of Tables with Captions -

Figure 1

Click here to access/download;Figure;Figure 1.tif

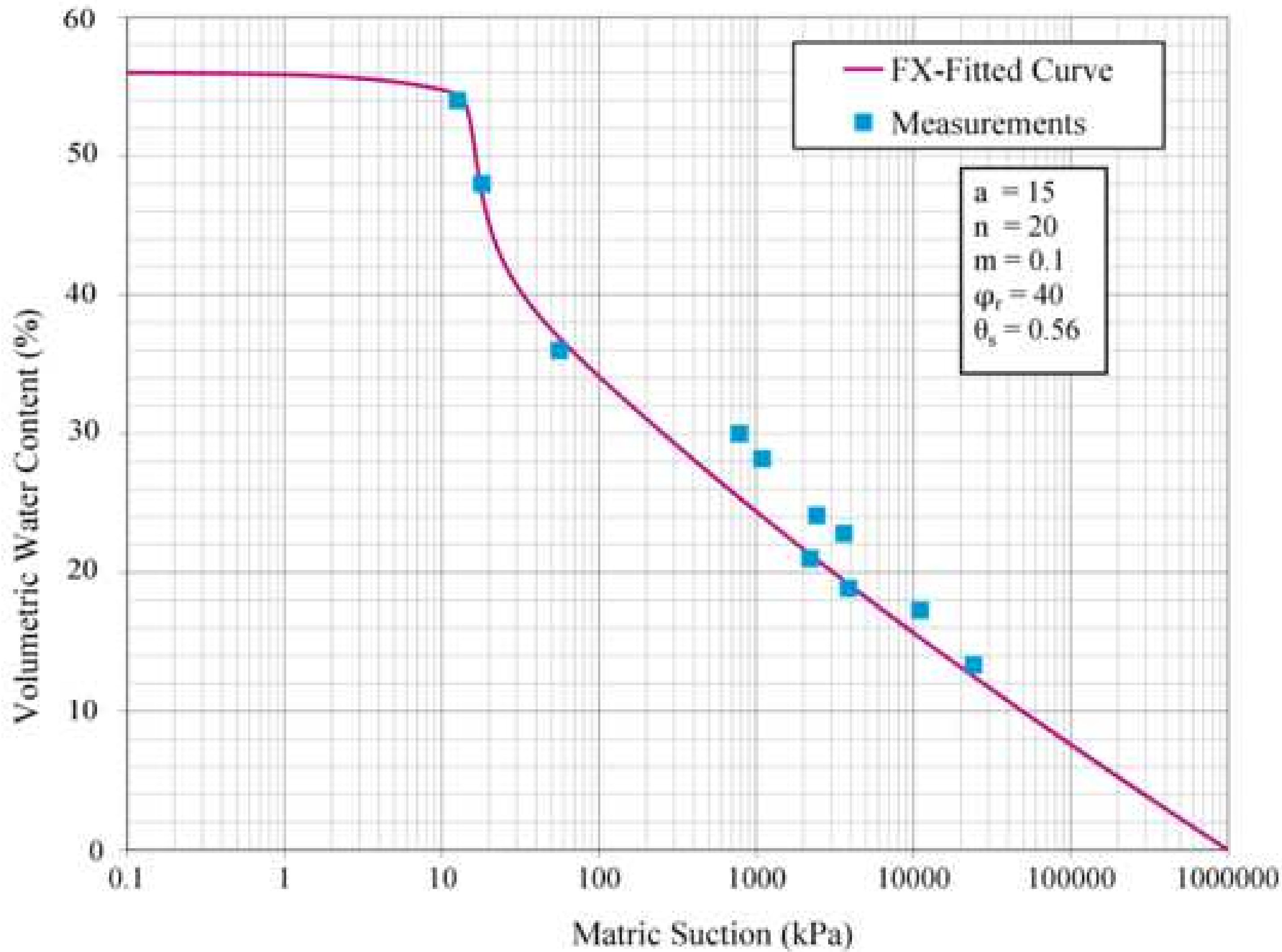

Figure 2 Click here to access/download;Figure;Figure 2.tif

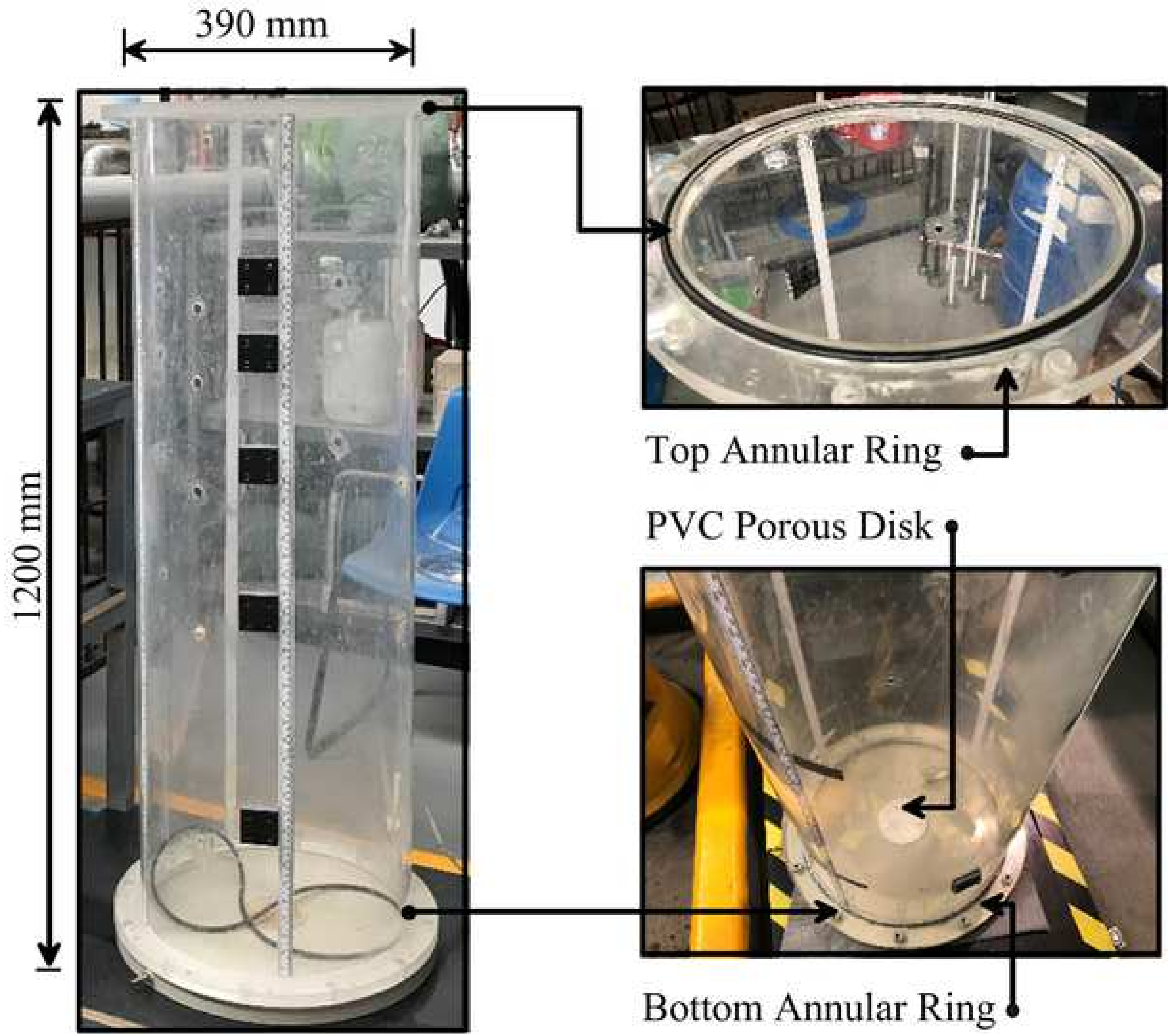

Figure 3

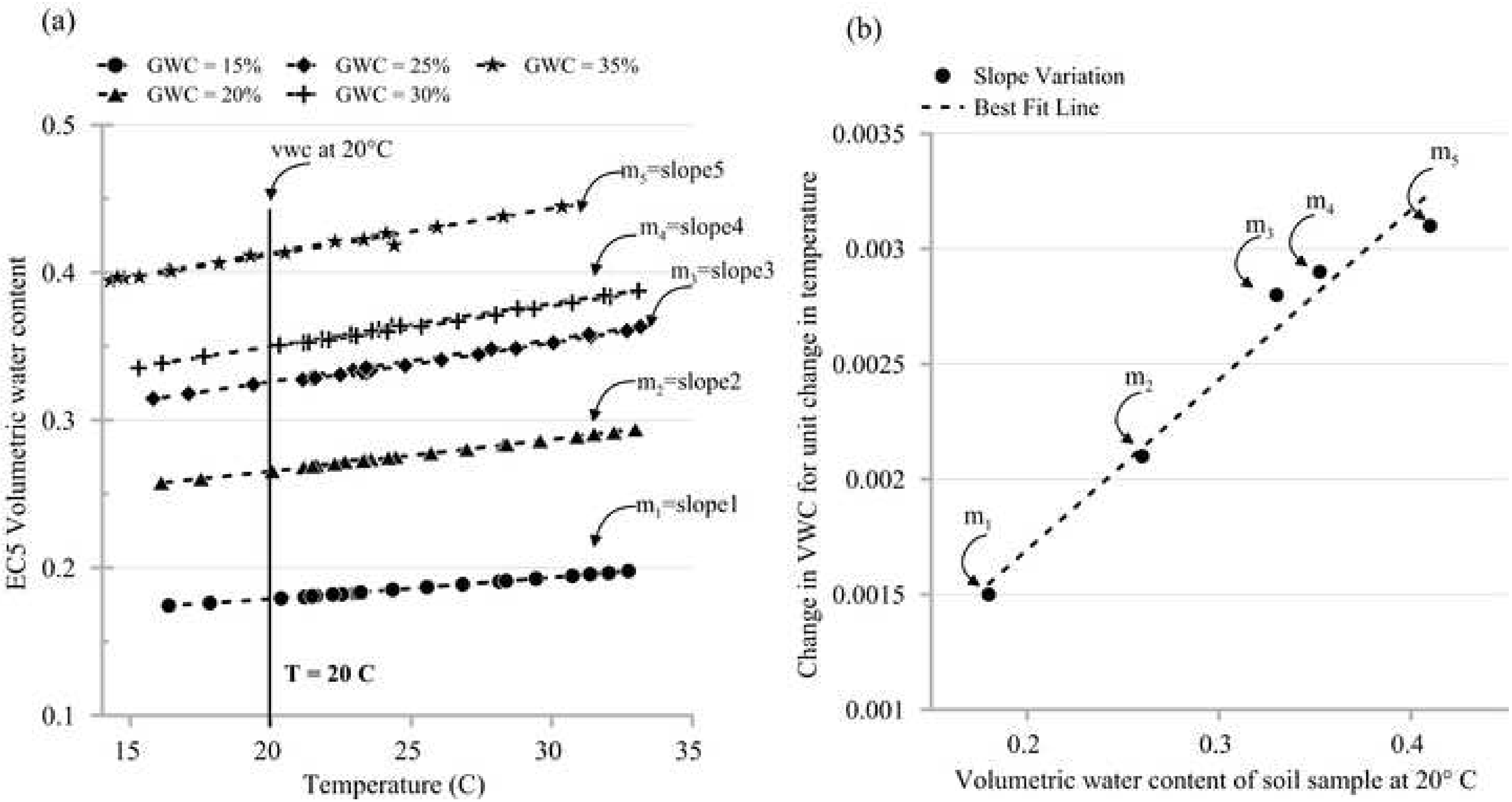

(a)
GWC = 15%
GWC = 20%
GWC = 25%
GWC = 30%
GWC = 35%
vwc at 20°C
m5=slope5
m4=slope4
m3=slope3
m2=slope2
m1=slope1
T = 20 C
EC5 Volumetric water content
0.5
0.4
0.3
0.2
0.1
15
20
25
30
35
Temperature (C)
(b)
Slope Variation
Best Fit Line
m5
m4
m3
m2
m1
Change in VWC for unit change in temperature
0.0035
0.003
0.0025
0.002
0.0015
0.001
0.2
0.3
0.4
Volumetric water content of soil sample at 20° C

Figure 4

Click here to access/download;Figure;Figure 4.tif

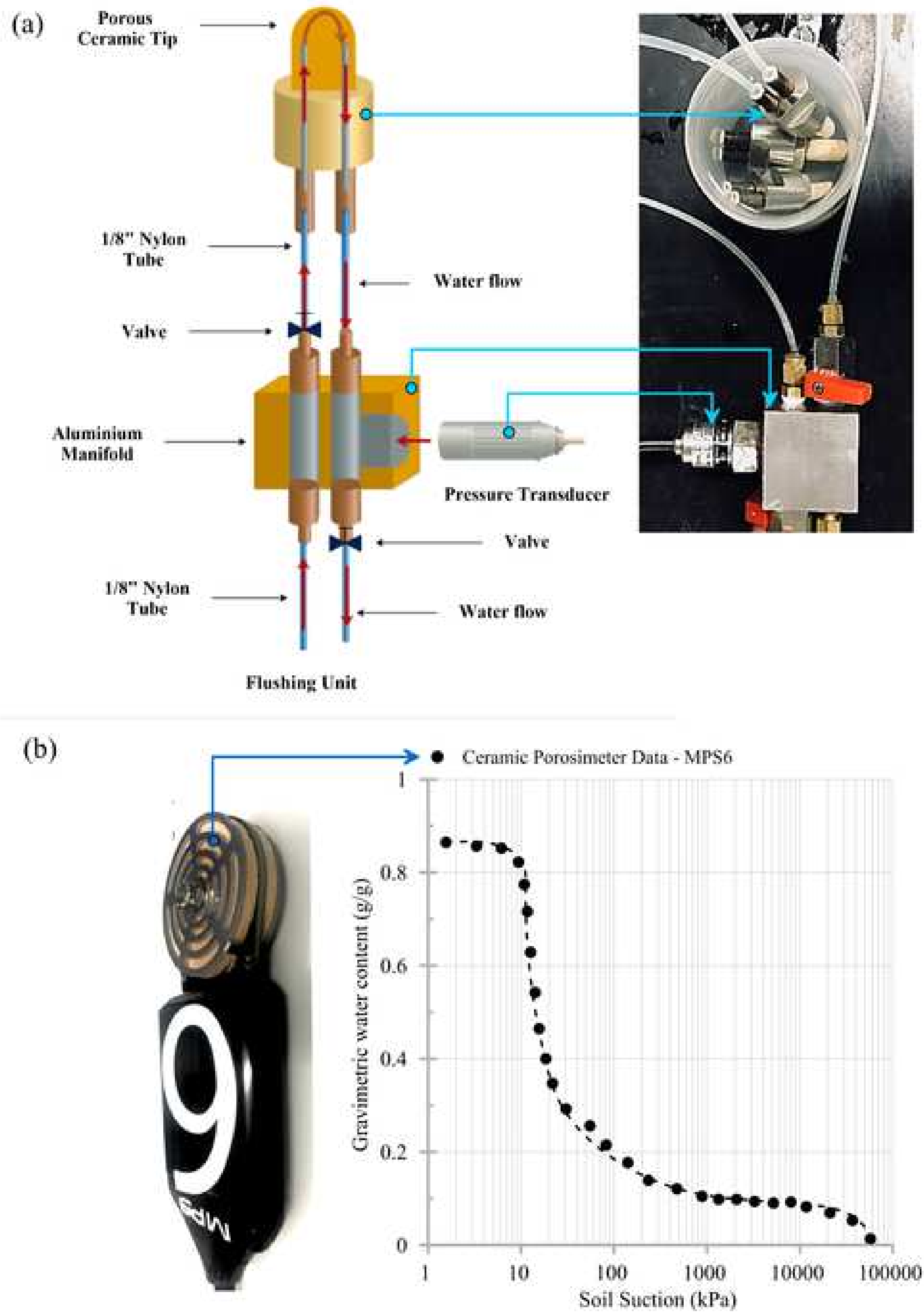

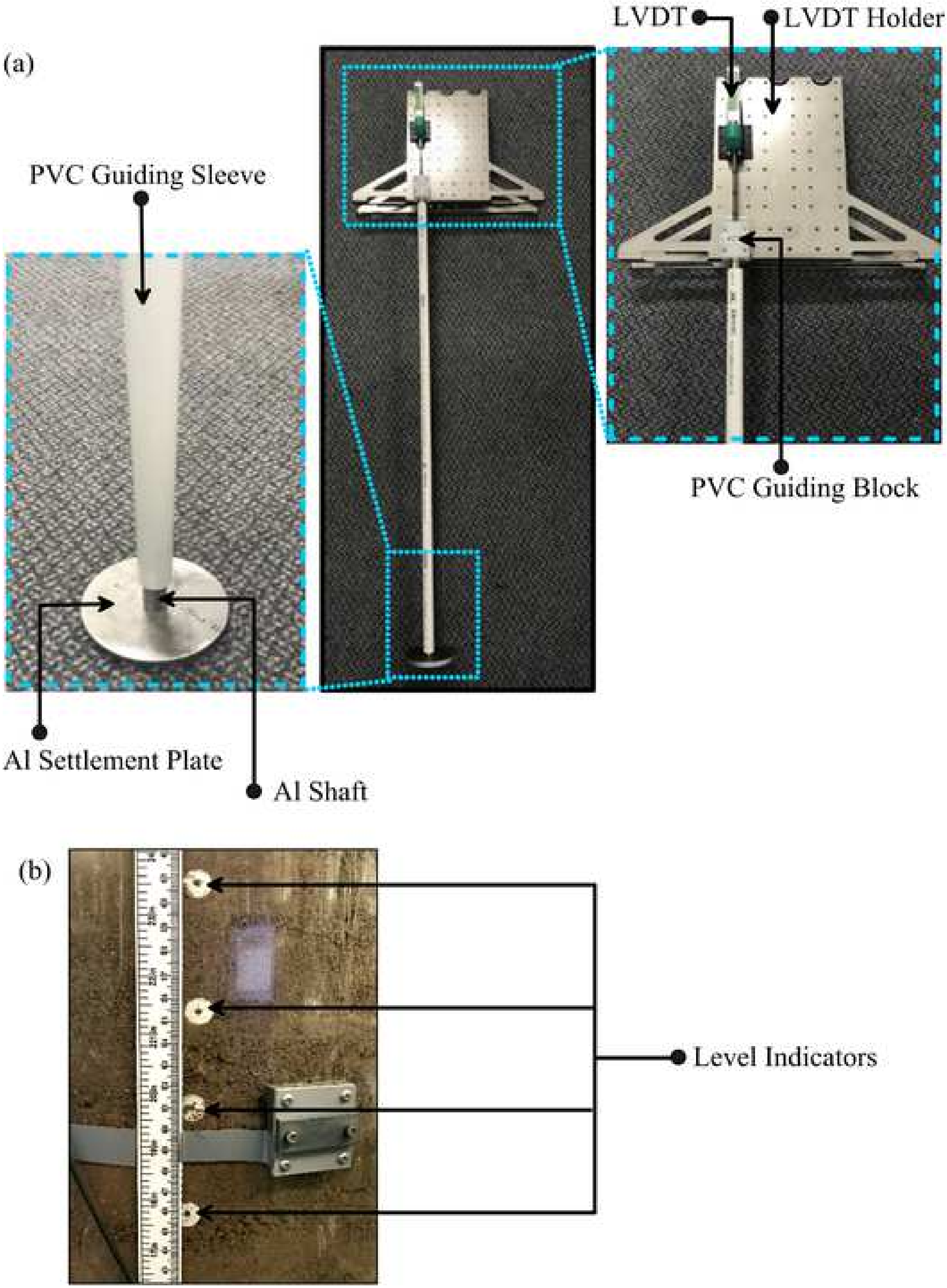
(a)
LVDT
LVDT Holder
PVC Guiding Sleeve
PVC Guiding Block
Al Settlement Plate
Al Shaft
(b)
Level Indicators

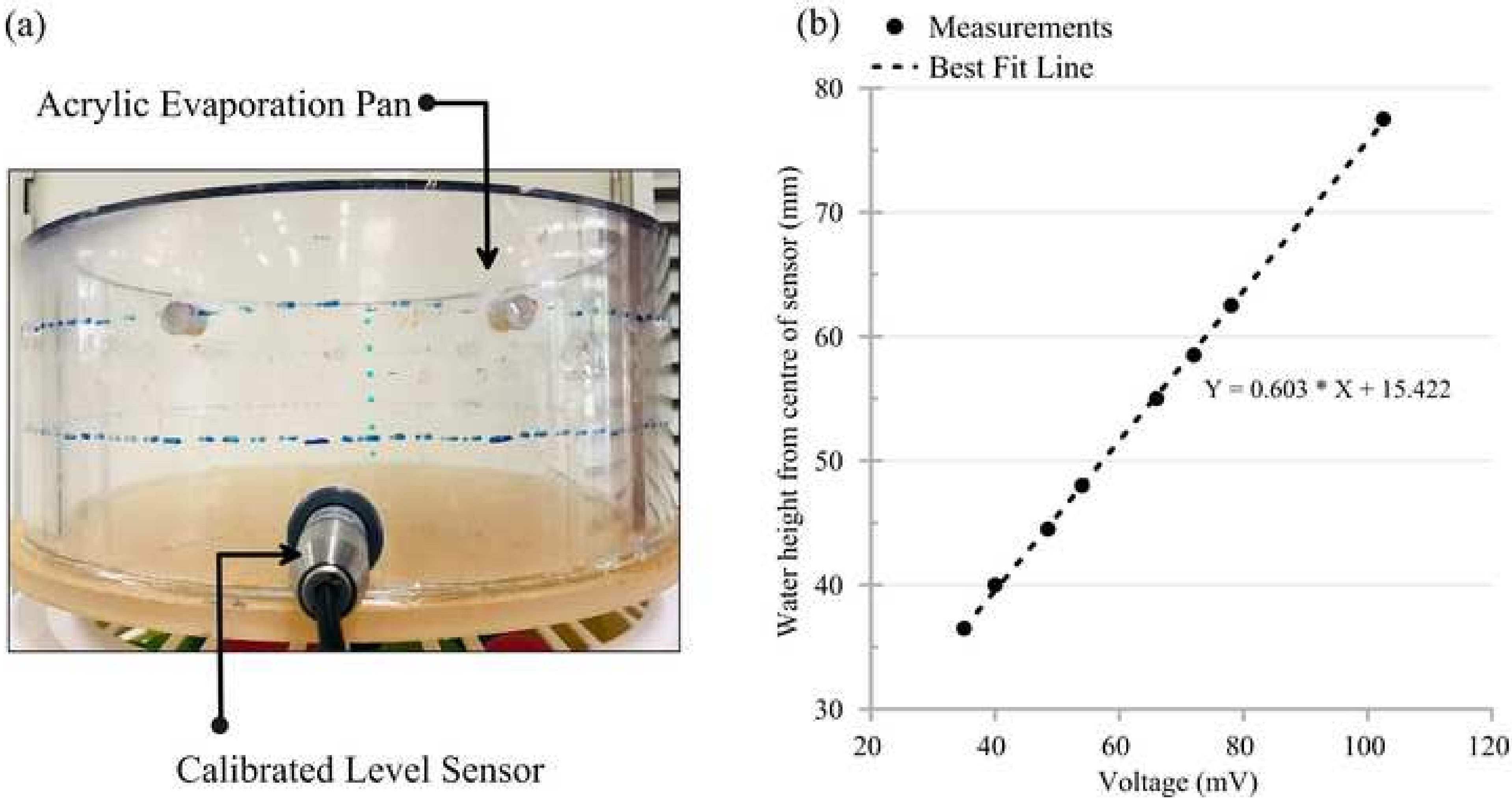
(a)
Acrylic Evaporation Pan
Calibrated Level Sensor
(b)
Measurements
Best Fit Line
Y = 0.603 * X + 15.422
Water height from centre of sensor (mm)
Voltage (mV)
80
70
60
50
40
30
20
40
60
80
100
120

Figure 7

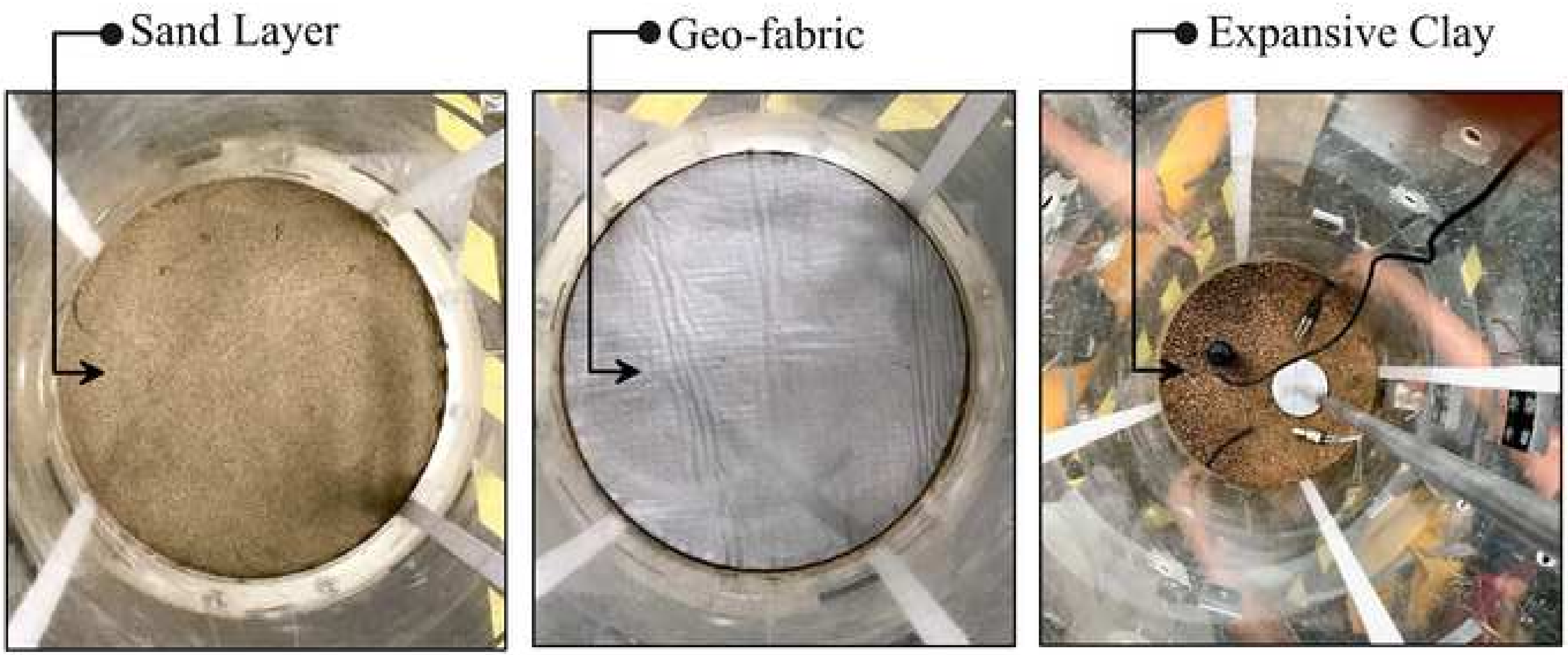

Figure 8

Click here to access/download;Figure;Figure 8.tif

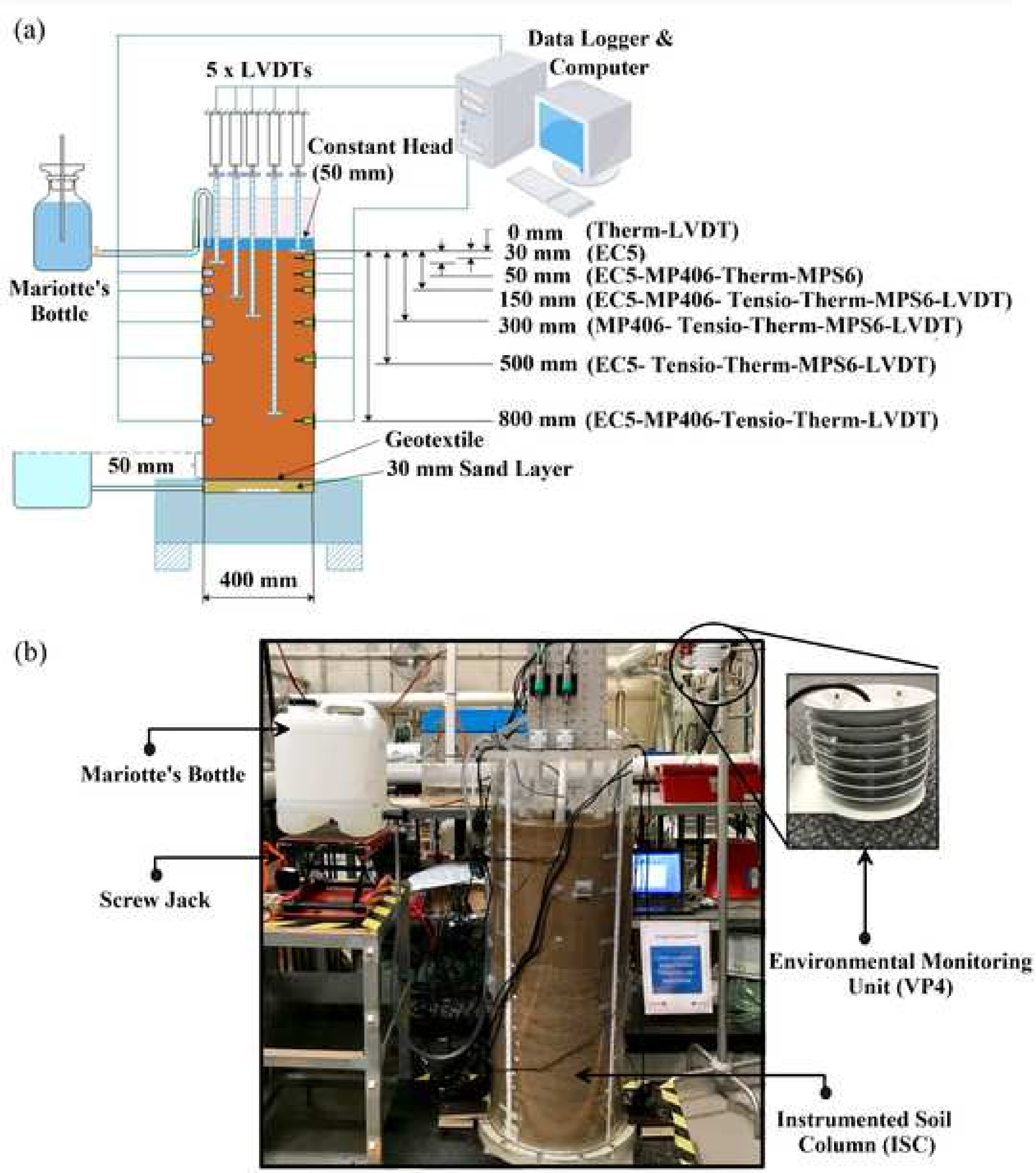

Figure 9

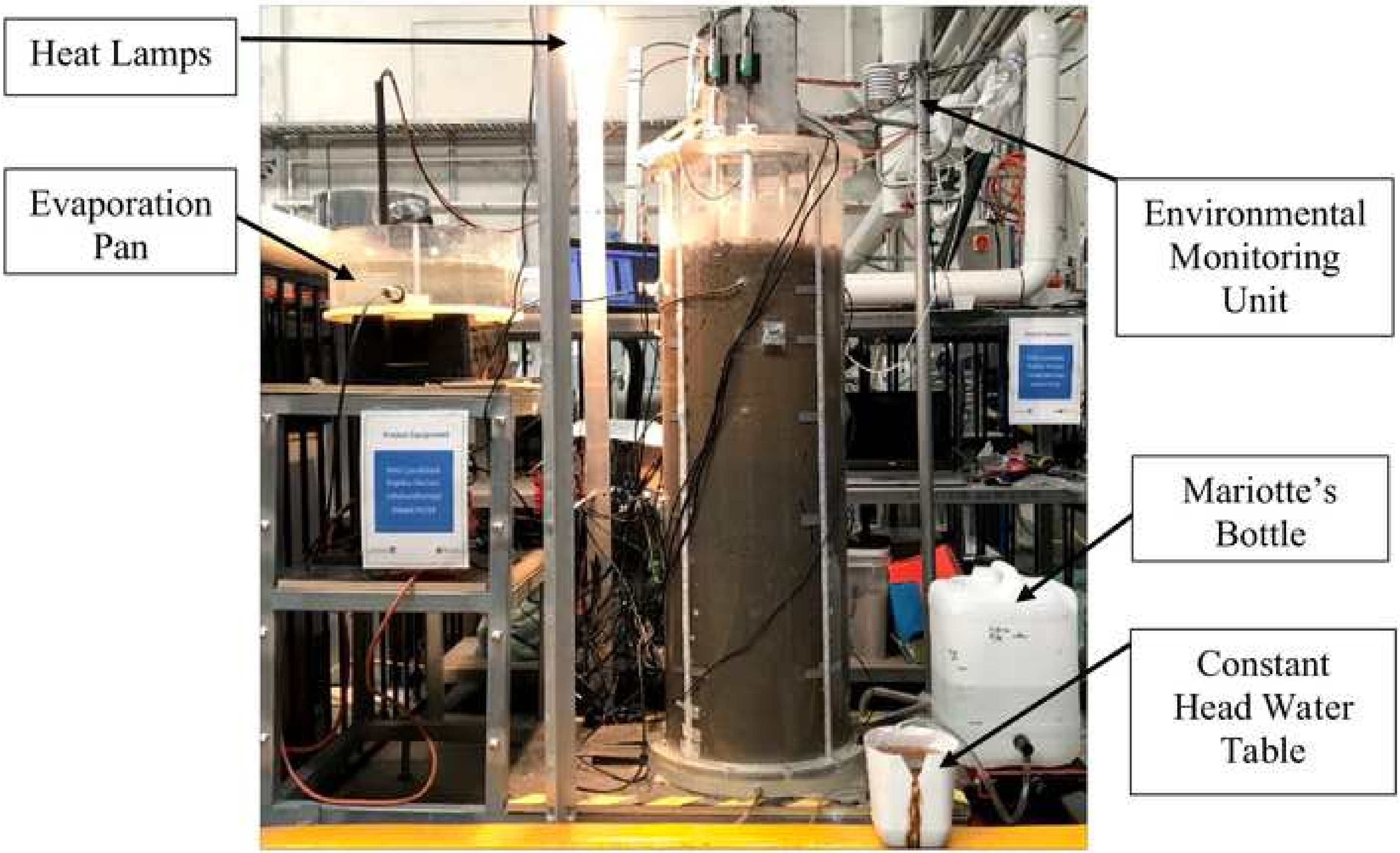
Heat Lamps
Evaporation Pan
Environmental Monitoring Unit
Mariotte's Bottle
Constant Head Water Table

Figure 10

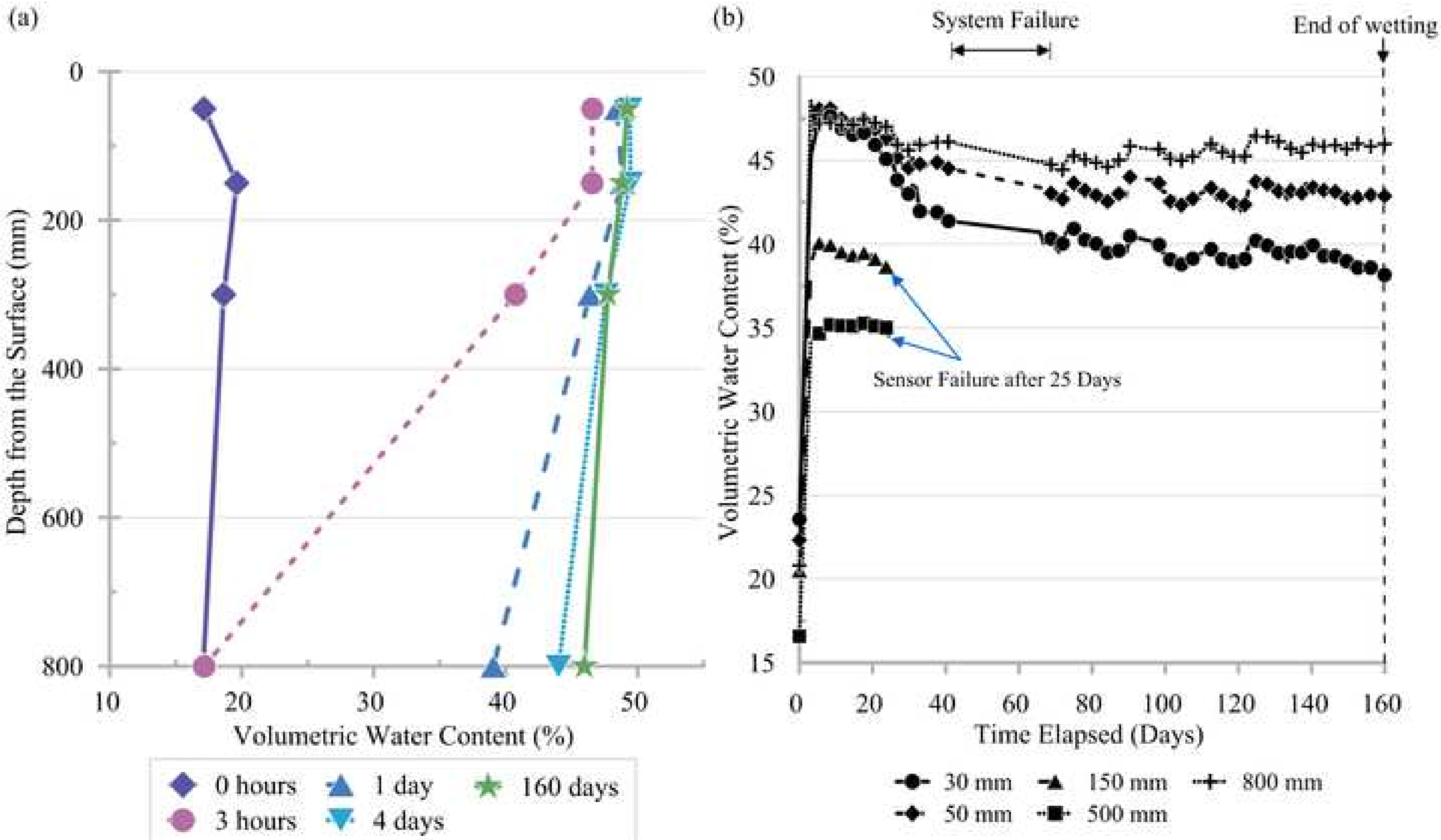

(a)
Depth from the Surface (mm)
0
200
400
600
800
10
20
30
40
50
Volumetric Water Content (%)
0 hours
1 day
160 days
3 hours
4 days
(b)
System Failure
End of wetting
Volumetric Water Content (%)
50
45
40
35
30
25
20
15
0
20
40
60
80
100
120
140
160
Time Elapsed (Days)
Sensor Failure after 25 Days
30 mm
150 mm
800 mm
50 mm
500 mm

Figure 11 Click here to access/download;Figure;Figure 11.tif

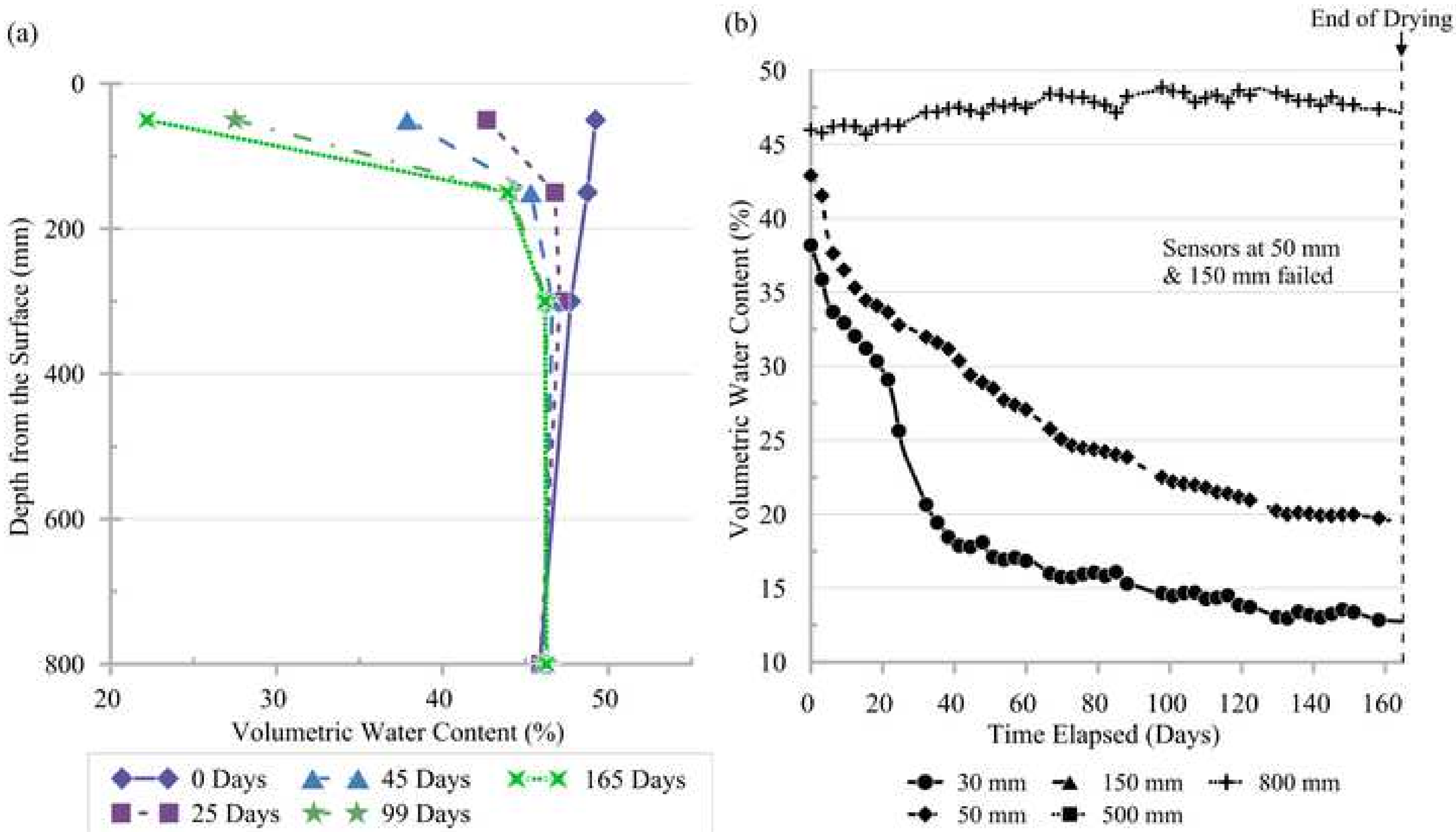

Figure 12

Click here to access/download;Figure;Figure 12.tif

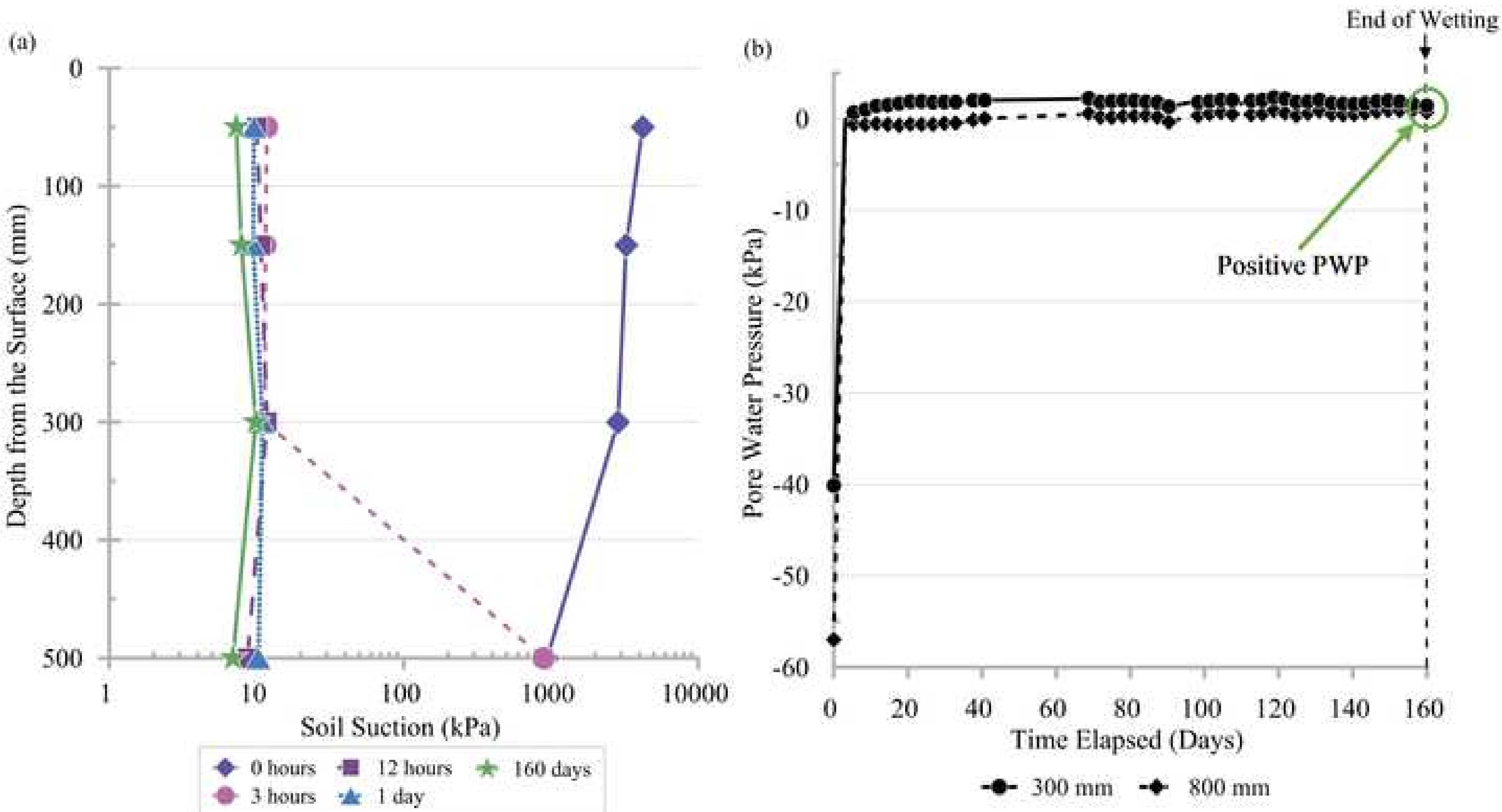

Figure 13 Click here to access/download;Figure;Figure 13.tif

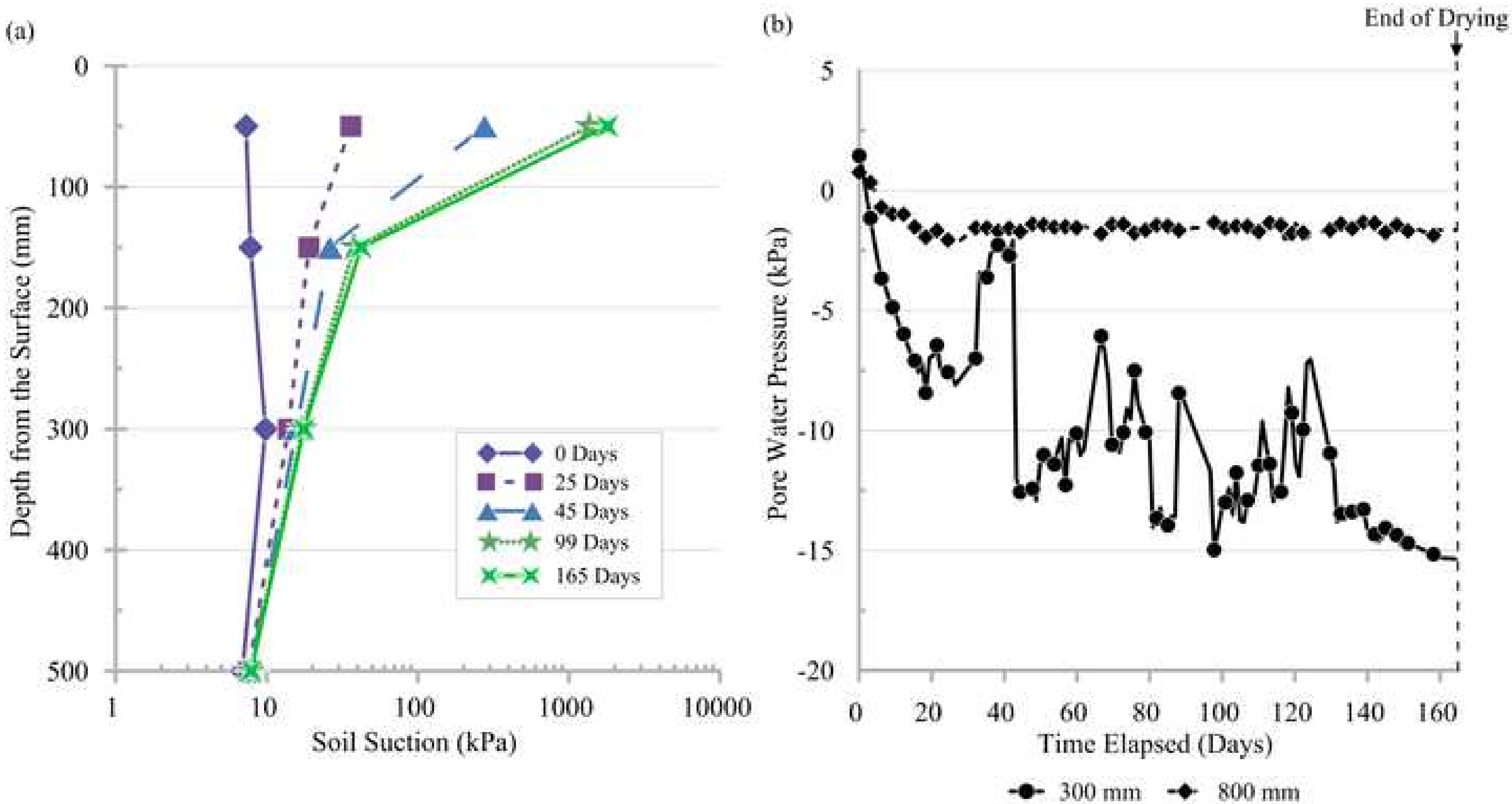

Figure 14

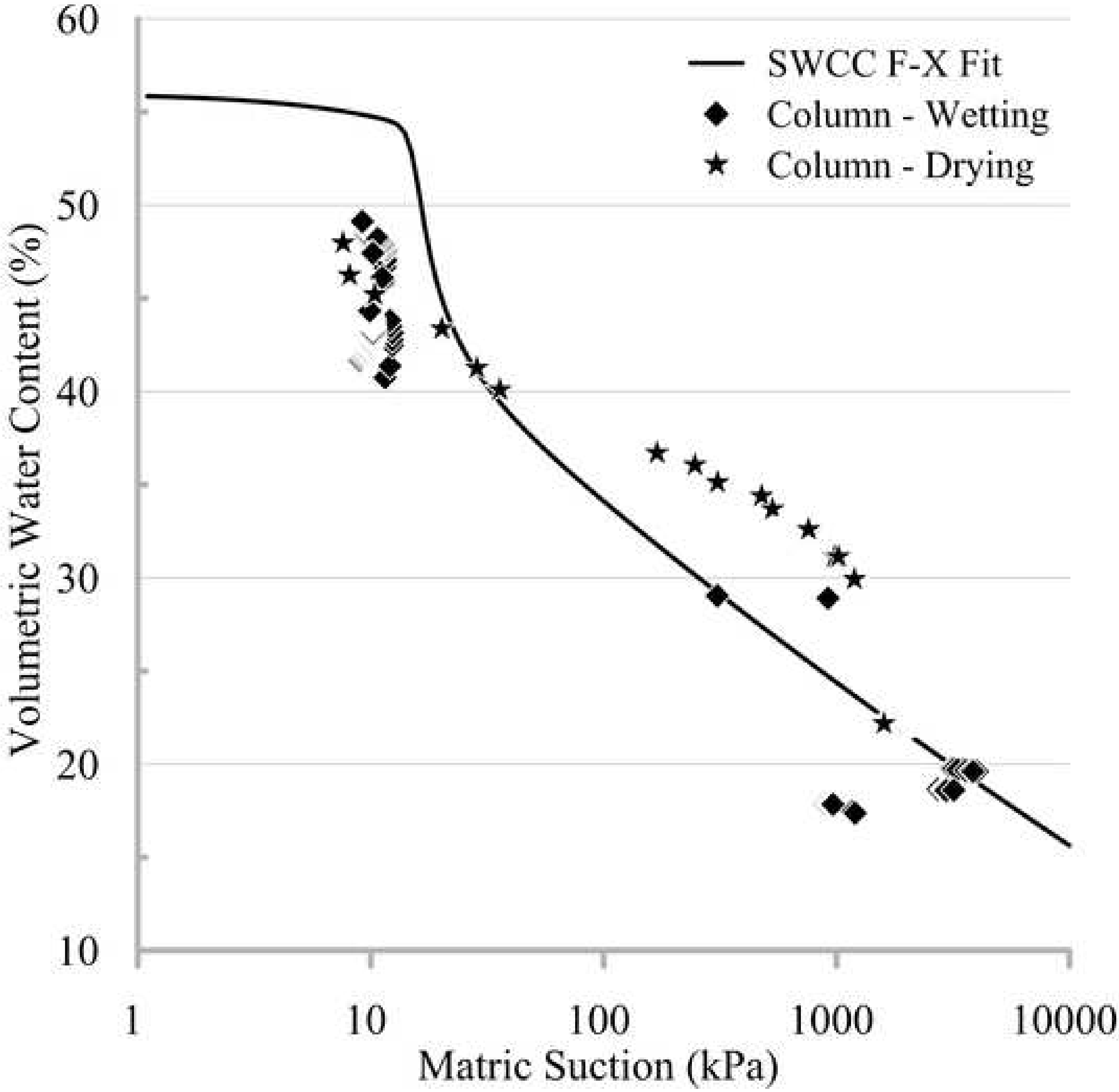
SWCC F-X Fit
Column - Wetting
Column - Drying
Volumetric Water Content (%)
60
50
40
30
20
10
1
10
100
1000
10000
Matric Suction (kPa)

Figure 15

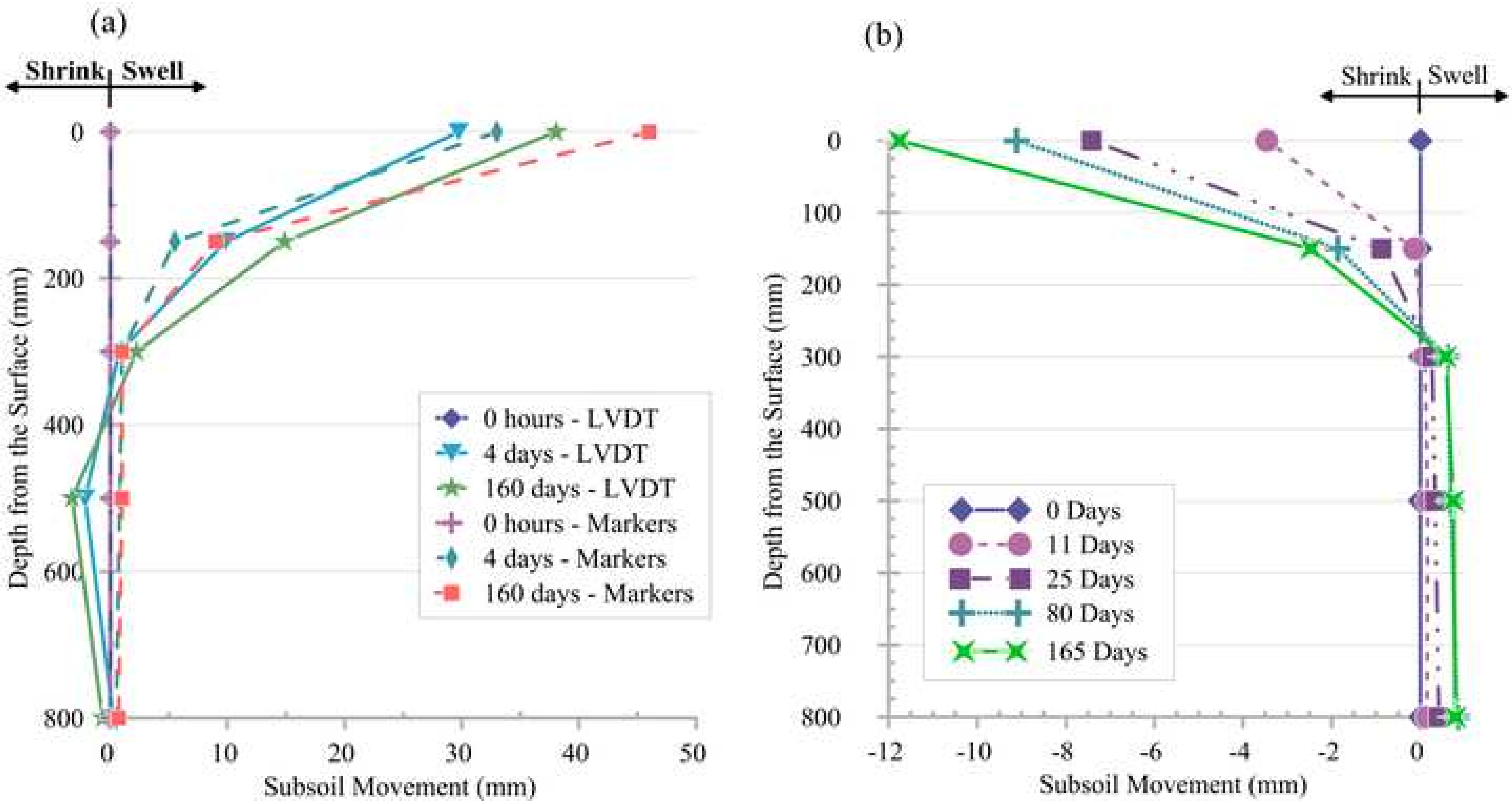
(a)
Shrink
Swell
0
200
400
600
800
0
10
20
30
40
50
Depth from the Surface (mm)
Subsoil Movement (mm)
0 hours - LVDT
4 days - LVDT
160 days - LVDT
0 hours - Markers
4 days - Markers
160 days - Markers
(b)
Shrink
Swell
0
100
200
300
400
500
600
700
800
-12
-10
-8
-6
-4
-2
0
Depth from the Surface (mm)
Subsoil Movement (mm)
0 Days
11 Days
25 Days
80 Days
165 Days

Classification Test	Results	Standard
Grain size distribution	% finer than 75μm > 77%	AS 1289.3. 6.3 (2003)
	Fraction of clay = 39 %	AS 1289.3.5.1 (2006)
Atterberg limits	LL = 67.0 %	AS 1289.3.4.1 (2008)
	PI = 37.2 %	AS 1289.3.1.1 (2009a)
Linear shrinkage	LS = 13.4 %	AS 1289.3.2.1 (2009b)
X-ray diffraction (XRD)	Smectite Group	
Specific gravity	G_s = 2.67	AS 1289.3. 6.1 (2009c)
Saturated hydraulic conductivity (compacted soil)	5×10^{-10} m/s	
Activity Value	0.95	

Depth from Surface (mm)	Types of Sensors & Embedded Depth					
	EC-5	MP406	Tensio	Therm-EP	MPS-6	LVDT
0				√		√
30	√					
50	√	√		√	√	
150	√	√	√	√	√	√
300		√	√	√	√	√
500	√		√	√	√	√
800	√	√	√	√		√
√ - Embedded Level for each Sensor